Unique Boron Carbide Nanoparticle Nanobio Interface: Effects on Protein-RNA Interactions and 3-D Spheroid Metastatic Phenotype

ROBERT K. DELONG[1], MIRANDA N. HURST[1], SANTOSH ARYAL[2] and NANTIPOOR K. INCHUN[3]

[1]*Nanotechnology Innovation Center of Kansas State (NICKS), Department of Anatomy and Physiology, Kansas State University, Manhattan, KS, U.S.A.;*
[2]*Nanotechnology Innovation Center of Kansas State (NICKS), Department of Chemistry, Kansas State University, Manhattan, KS, U.S.A.;*
[3]*Department of Biological Sciences, Louisiana State University, Shreveport, LA, U.S.A.*

Abstract. *Aim: The effect of boron carbide (B_4C) nanoparticles (NP) on protein-RNA complexes and metastatic phenotype of 3-D tumor spheroids was investigated. Materials and Methods: Characterization was performed by transmission electron microscopy (TEM), zeta potential (ZP), 2-dimensional fluorescence difference spectroscopy (2-D FDS), gel electrophoresis, MTT, haemolysis and 3-D tumor spheroid assays. Results: TEM showed NP were homogenous (≤50 nm) and spherical in shape. Zeta potential (ζ) of NP (-43.3) shifted upon protein:RNA interaction (+26.9). Protein:RNA complex interaction with NP was confirmed by 2-D FDS, demonstrating excitation/emission blue shift and lowered fluorescence intensity, and electrophoretic mobility shift assay (EMSA), where presence of B_4C ablated visualization of the complex. B_4C NP cytotoxicity was less than zinc oxide by MTT assay, protected haemolysis and effected 3-D tumor spheroid metastatic phenotype. Conclusion: Nanobio interface of B_4C nanoparticles is unique and its anticancer potential may be mediated by altering protein and RNA interactions.*

Nanoparticles are being developed for a wide variety of industrial, research and medical applications. The RNA nanobio interface is poorly understood and has not yet been investigated as a cancer therapy. Ironically for boron carbide (B_4C) nanoparticles, despite this material being one of the hardest in nature, its unique nanobio properties are unknown. Biomedical applications for B_4C nanoparticles have thus far focused only on neutron-guided or T cell-adopted immunotherapies (1-3), rather than anticancer mechanisms and activity, that was the focus of the present study.

Direct and selective anticancer activity for metal oxide nanoparticles such as zinc oxide and cobalt oxide is known (4-9). The anticancer mechanism for these types of nanoparticles has been shown to be due to ROS and the induction of apoptotic signaling, rather than mediation or ablation of RNA-protein interactions. Interaction of RNA including the anticancer polyinosinic-polycytidilic acid (poly IC) to other metal oxide nanoparticles of biomedical interest, such as iron oxide and manganese oxide, requires polymer complexation or functionalization (10-12). However no prior work has been performed to characterize naked boron carbide (B_4C) nanoparticle interaction to RNA-protein complexes.

Zeta potential analysis is commonly performed to verify electrostatic interaction between the nanoparticle and protein or RNA, where a shift in the particle surface charge is observed (12, 13). Herein, interaction of the B_4C nanoparticle to poly IC:protamine complexes has been shown by zeta potential (ZP) analysis, and by changes in the 2-D FDS or electrophoretic pattern of the RNA-protein complexes. Finally, cell bio-activity of the B_4C nanoparticles was assessed by MTT assays and by their effect on the metastatic phenotype of B16-F10 mouse melanoma or HeLa cells cultured in 3-D tumor spheroid models.

Materials and Methods

Materials. Boron carbide (B_4C) nanoparticles were obtained from Plasma Chem (Berlin, Germany). Protamine Sulfate and Poly IC (Polyinosinic: polycytidylic acid) were obtained from Sigma Aldrich (St. Louis, MO, USA).

This article is freely accessible online.

Correspondence to: R.K. DeLong, Nanotechnology Innovation Center of Kansas State (NICKS), Department of Anatomy and Physiology, Manhattan, KS 66506, U.S.A. Tel: +1 7855326313, Fax: +1 7855324953, e-mail: robertdelong@ksu.edu

Key Words: Tumor spheroid, 2-dimensional fluorescence difference spectroscopy (2-D FDS), zeta potential (ZP), boron carbide nanoparticle (B_4C NP), polyinosinic: polycytidylic acid (poly IC).

Transmission electron microscopy. TEM was conducted essentially as previously described (13) on a FEI Technai G2 Spriti BioTwin (FEI, Hillsboro, OR, USA) equipped with a HAADF detector for STEM imaging at 120 keV.

Zeta potential. Zeta Potential analysis was conducted as previously described (12, 13). Nanoparticle or protein-RNA complexes were suspended in water and mixed 1:1 vol/vol and analyzed directly on the Malvern Zetasizer Nano ZSP (Worcestershire, England, UK). Zeta potential cuvettes were purchased from Malvern.

Gel electrophoresis. Protamine (1 mg/ml) and pIC RNA (1 mg/ml) were dissolved in double-distilled water and mixed in 1:1 vol/vol and loaded directly with 6× loading buffer (New England Biolabs, Ipswich, MA, USA), electrophoresced through 1% agarose and stained with DNA safestain (MidSci, St. Louis, MO, USA). The gel was imaged on a Bio-Rad Molecular Imager Gel Doc XRT imaging system (Hercules, CA, USA).

2-D FDS. 2-D FDS Experiments were conducted on a Molecular Devices Spectramax i3x instrument equipped with SoftMax Pro 6.4.2 software (Sunnyvale, CA, USA) using the Spectral Optimization Wizard. 0.5 mg/ml nanoparticle was sonicated briefly and scanned directly or added to protein-RNA complexes 1:1 vol/vol and scanned immediately. Excitation frequencies were scanned from 250 to 500 nm. Emission frequencies were recorded from 300 to 700 nm. Relative fluorescence intensities ranged from 86 to 111.5.

MTT assay. NIH3T3 or A375 cells approaching confluency were trypsinized, rinsed twice with PBS, pelleted by centrifugation and re-suspended at approximately 5,000 to 8,000 cells per 0.3 ml 10% FBS/DMEM media and allowed to plate overnight. Dulbecco's Modified Eagle Medium (DMEM) and lipofectamine 2000 were purchased from Thermo Scientific (Waltham, MA, USA), and fetal bovine serum (FBS) was purchased from Midsci (St. Louis, MO, USA). The media was then aspirated and nanoparticles suspended at 25 μg/ml in 10% FBS indicator-free DMEM with and without lipofectamine (20 μg/ml). The cells were maintained at 37˚C and 5% CO_2 for an additional 24 h with exposure to nanoparticle treatment after which they were washed once with PBS and received 5 mM MTT solution for 4 h. Afterwards all except 25 μl were removed and 50 μl DMSO was added for 10 min and absorbance was read at 562 nm on a Spectramax Paradigm (Molecular Devices, Sunnyvale, CA, USA). Data plotted represent the mean of more than 3 wells as a percentage of control cells receiving no treatment.

Cell morphology. Cells were trypsinized and adjusted to 1.2×10^5 cells/ml and plated onto sterile CoStar 6-well cell culture dishes (Fisher Scientific, Waltham, MA, USA). Cells were allowed to adhere overnight in the cell incubator at 37˚C and 5% CO_2 and were treated the next morning with 0.01 or 0.05 mg/ml NP and imaged at time zero, 36 and 72 h at 10× or 20× magnification using an inverted microscope (Olympus, Model# CKX41, Center Valley, PA, USA) with camera attachment (Olympus, Model# SC100, Center Valley, PA, USA).

Hemolysis assay. Blood haemolysis assay is a simple measurement of haemoglobin release due to disruption in red blood cells. In a typical procedure, red blood cells (RBC, 1 ml) were purified by repeated centrifugation at 2,000 rpm for 5 min to remove plasma and any buffy coats. Purified RBCs were then redispersed in PBS (1 ml) and incubated with boron carbide (1 mg/ml) nanoparticles pre-dispersed in PBS for predetermined time intervals (0, 15, 30, and 60 min, 100 rpm using orbital shaker) at 37˚C. After each time interval, RBCs were pelleted gently and the supernatant was subjected to spectrophotometric analysis at the range of 300 to 500 nm. Characteristic haemoglobin absorption maximum (410 nm) was taken as reference for qualitative haemolytic assessment. Control samples were treated side-by-side to test samples.

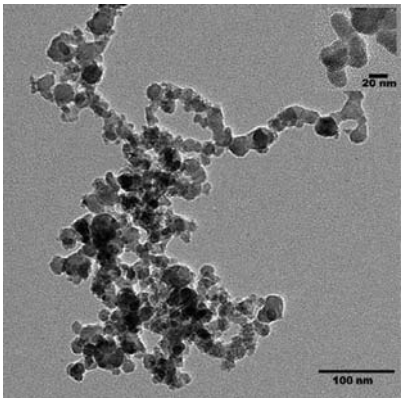

Figure 1. *Morphology of B_4C nanoparticles imaged by TEM.*

Spheroid assay. For both assays, NP were washed in water, 100% ethanol, 70% ethanol, and centrifuged at 14,000 rpm for 20 min decanting the supernatant in between each rinse. NP tubes were brought into the cell culture hood, and left under UV light for 30 min to sterilize prior to suspending in indicator free DMEM. Spheroids were grown in a 96 well Insphero Gravity TRAP™ ULA plate (Perkin Elmer, Waltham, MA, USA). The plates were dampened with 40 μl of media followed by aspiration prior to inoculation. 1,000 cells/ml (HeLa) or 5,000 cells/ml (B16F10) were inoculated per well, plates were centrifuged at 2,200 rpm for 3 min and allowed to incubate at 5% CO_2 and 37˚C for 24 h prior to treatment with 50 μg/ml in well concentration of B_4C NP. Cells were maintained in 10% FBS/DMEM supplemented with 1% Penicillin-Streptomycin (Thermo Scientific, Waltham, MA, USA).

Results

Nanoparticle characterization. The size and shape of the B_4C nanoparticles was determined by TEM imaging. These data are shown in Figure 1. As can be seen in Figure 1, B_4C NP were spherical in shape and relatively homogenous with respect to morphology. B_4C NP were small with the majority population less than 50 nm in diameter and in many cases less than 30 nm.

B_4C nanoparticles bind protamine:poly IC complexes. Protamine is a cell-penetrating peptide (CPP) that we and others have shown binding to DNA and RNA to form

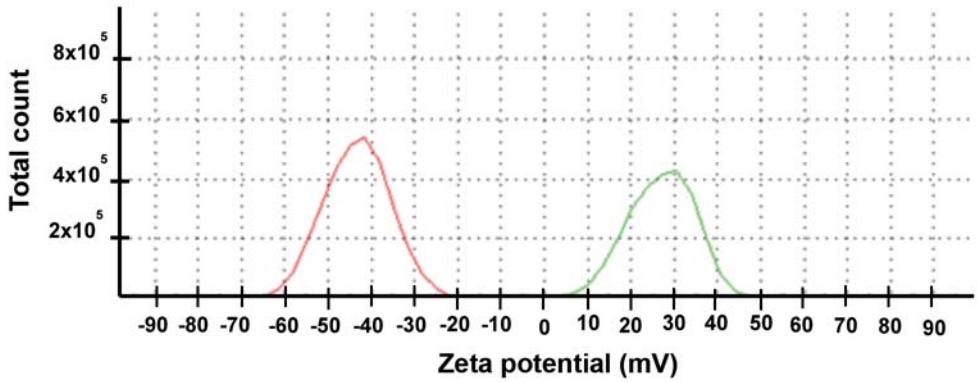

Figure 2. *Evidence of B_4C nanoparticle interaction to RNA-protein complexes by zeta potential analysis.*

nanocomplexes helping to stabilize and deliver the nucleic acids (14-19). Poly IC, polyinosinic:polycytidylic acid, is an anticancer double-stranded RNA (dsRNA) molecule (20), which has been recently shown to possess anti-metastatic properties (21-23). Herein we complexed protamine to poly IC and detected the ensuant nanocomplexes and their interaction to B_4C NP by zeta potential analysis. These data are shown in Figure 2. The zeta potential (ζ) as a measure of charge at or near the surface of the NP was highly negative for B_4C NP (-43.3 mV). Although these measurements were obtained in water, B_4C NP gave significantly negative ZP value (-37 mV) in phosphate buffered saline at pH 7.4 as well (data not shown). Previously we had observed that protamine:RNA complexes tend to favour a higher ratio of protamine to RNA (24), where multiple peptides could associate along the strand of the RNA polymer. Thus, it was not surprising that interaction of B_4C NP to the protamine:poly IC complex is greatly shifted in the positive direction (+26.9 mV). Somewhat surprising however was that the B_4C NP population completely shifted rather than seeing a partial peak for uncomplexed B_4C where only one population was observed suggesting B_4C NP-protamine:poly IC ternary complexes. Based on our experience with other nanoparticles and their biomolecular complexes (12, 13), this is unusual and likely reflects the unique nanobio interface of B_4C NP.

B_4C nanoparticles ablate protamine:poly IC complexes by gel electrophoresis. Gel electrophoresis mobility shift assay is commonly used to detect protein-RNA interaction (24). Previously we observed protamine to complex RNA (tRNA) to form nanoparticles (14), and when the RNA was stained by ethidium bromide, the protamine:RNA complex could be detected by gel electrophoresis. Here we applied this technique to detect protamine:poly IC RNA complexes, where DNA safestain dye was used to detect either the RNA or protein:RNA complex. These results are shown in Figure 3. As shown in Figure 3, as expected in lanes 2 and 3 respectively, poly IC being an RNA anionic polymer migrates toward the cathode and the highly cationic protamine CPP migrates towards the anode and the protein-RNA complex is intermediate. In the presence of zinc oxide nanoparticle, some loss in the protein:RNA complex is observed consistent with its protamine interaction (13), and

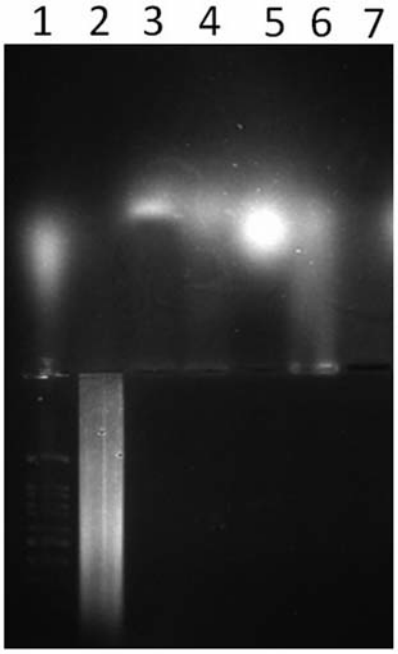

Figure 3. *EMSA analysis of poly IC, protamine, its complexes and ablation by B_4C NP. DNA ladder (lane 1), Poly IC (lane 2), Protamine (lane 3), Protamine:Poly IC complex (lane 4), DNA safestain (lane 5), Protamine:Poly IC complex + control nanoparticle zinc oxide (lane 6), Protamine:Poly IC complex + B4C nanoparticle (lane 7).*

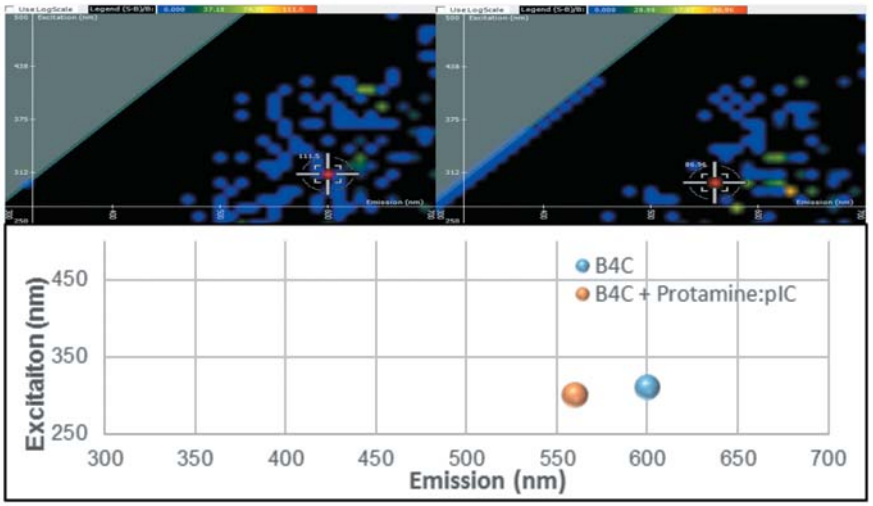

Figure 4. *2-D FDS of B_4C nanoparticle (left) or B_4C-protamine: RNA complex (right). Composite plot (bottom).*

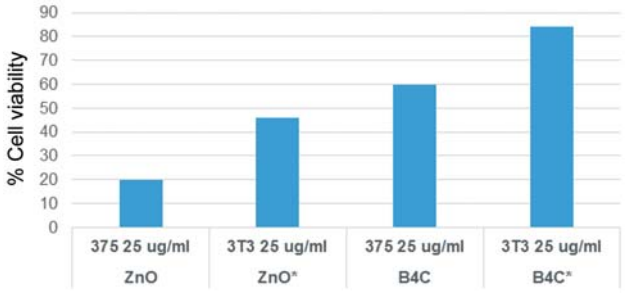

Figure 5. *Effect of ZnO (control) or B_4C nanoparticles on cell (A375 or NIH3T3) viability by MTT assay.*

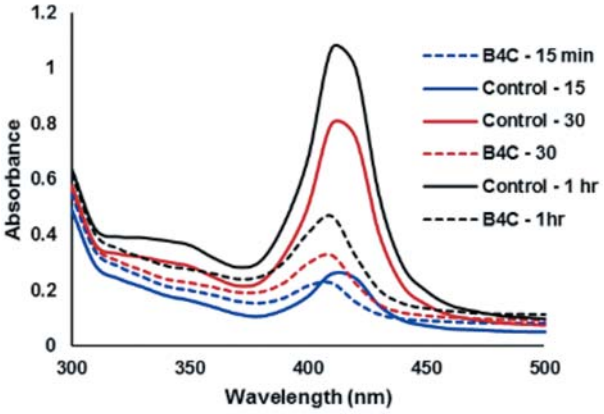

Figure 7. *Hemolysis assay time course for exposure to B_4C nanoparticle.*

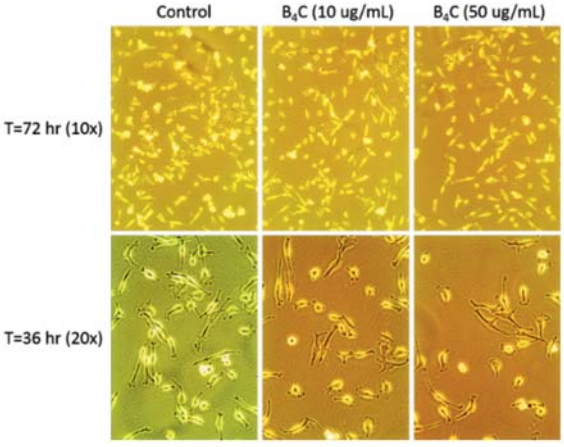

Figure 6. *Effect of B_4C nanoparticles on HeLa cell morphology. 10x-72 h (top) or 20×- 36 h (bottom).*

the concomitant release of the RNA from the complex as expected. However strikingly, the complete loss of any staining was shown in the presence of B_4C nanoparticle. In this case B_4C nanoparticle ablated the protein:RNA complex as can be seen by comparing the pattern of lane 7 to either lane 6 (complex with ZnO NP) or lane 4 (complex alone). These data were unexpected and again suggest that the nanobio interface of B_4C nanoparticle is unusual.

Fluorescence difference spectroscopy analysis confirms protein and RNA nanobio interface. Previously we described high-throughput fluorescence difference spectroscopy characterization of liposome surface interaction with nanoparticles (25). Here we used 2-dimensional fluorescence

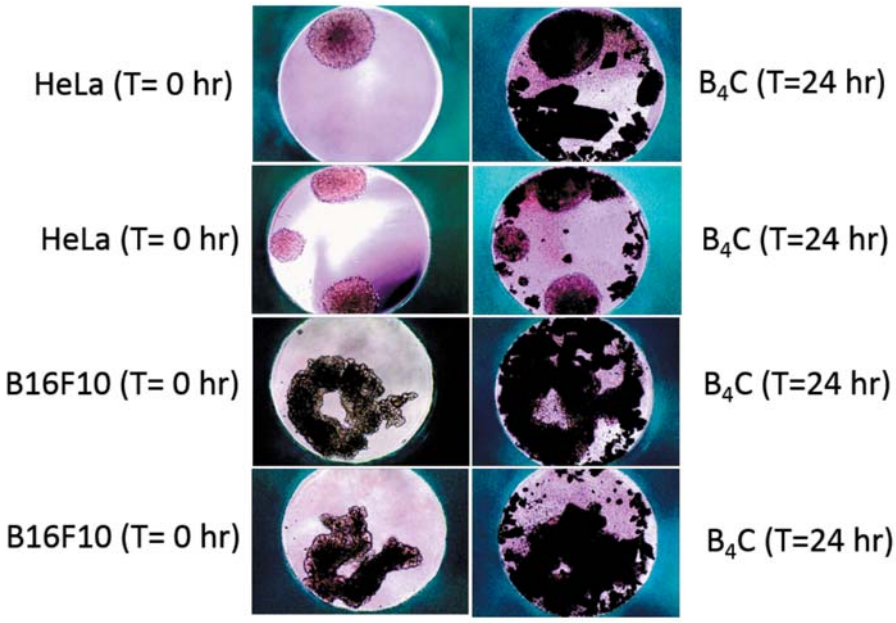

Figure 8. *Effect of B_4C nanoparticle on metastatic phenotype of Hela or B16F10 3-D spheroid cultures.*

difference spectroscopy (2-D FDS) to characterize the B_4C nanoparticles and their interaction with protamine:poly IC complexes plotting fluorescent intensity per excitation and emission intersect.

As shown in Figure 4, B_4C NP exhibited fluorescence at about 308-310 nm excitation and an emission wavelength of approximately 600 nm. A significant blue shift occurs, however, when the NP binds to the protamine:poly IC RNA and protein complex, where due to the energy transfer and quenching that occurs at the surface, the maximal fluorescent intersect detected emitted at 570-580 nm with a concomitant decrease in intensity. Thus, the 2-D FDS pattern confirms nanobio interaction of B_4C nanoparticles supporting the prior zeta potential determinations. A drop in the intensity of the B_4C NP fluorescence also suggests surface interaction of the protein:RNA complex.

Effect of B_4C nanoparticles on cell viability. Previously we tested the cytotoxic effect of nanoparticles on A375 human melanoma cells by the MTT assay (26). Herein we wished to test the cytotoxicity of B_4C nanoparticles by MTT assay similarly, but were interested in comparing the results to an untransformed control cell line (NIH3T3). In this experiment we used zinc oxide (ZnO) nanoparticles as a control for which we have previous cytotoxicity information albeit using other assays and other cells (13). These data are shown in Figure 5. As can be seen in Figure 5, within the error range of these experiments (+/– 5%), the cell toxicity of B_4C was comparatively less than that of ZnO nanoparticles. Surprisingly, cytotoxicity of the nanoparticles was less for NIH3T3 cells than for A375. This is consistent with selective melanoma cell killing we and others have observed for ZnO NP, but importantly here extended to B_4C nanoparticles.

Effect of B_4C nanoparticles on cell morphology. Next the effect of the nanoparticle treatment on cell morphology was examined by light microscopy. These data are shown in Figure 6. As can be seen in Figure 6, no overt effect on the morphology of HeLa cells was observed. Certain kinds of nanoparticles are well-known to trigger apoptosis and this causes cells to round-up, swell and become birefringent. Clearly no such bio-activity was evident, even under relatively high concentrations (50 μg/mL) of B_4C nanoparticle treatment.

Cell Bio studies. Hemolysis assay is often used for nanoparticles or functionalized nanoparticles to gauge their cell membrane penetration and/or lysis of cells. These data are shown for B_4C nanoparticle in Figure 7. As shown in Figure 7, hemolysis assay is the observation of release of hemoglobin from red blood cells (RBC). As can be seen above the characteristic absorbance of hemoglobin (Hb) at 410 nm increases with the incubation time showing the loss of cell membrane integrity. The extent of loss of membrane integrity is higher in control RBC without any nanoparticle when incubated under the same conditions. During the 15-min time point there is no significant difference in the hemolysis, however, interestingly at later time points, the

control group showed a significant release of hemoglobin as that of treated one. This suggests that the B_4C nanoparticle delays increase in Hb that is associated with lysed cells or reduced maintenance of the cell membrane. The enhancement in the stability of RBC in presence of NPs presumably due to the presence of highly negative charged particles (-37 mV, Figure 5B) at the vicinity and interfaces of RBC prevent the colloidal instability and inter RBC fusion during mechanical shaking. Note that RBCs used in hemolysis experiment are purified to remove serum proteins, which helps in stabilizing RBC in higher mechanical stress. On the other hand, the control RBCs hemolysis under the experimental condition is most probably due to the collision between the RBCs, thereby, enhancing membrane fusion, which ultimately alters membrane integrity. This is interpreted positively for the cell biology activity of B_4C nanoparticles.

Effect of B_4C nanoparticles on metastatic phenotype in 3-D spheroid models. Recently 3-D spheroids have been reported as models of avascular metastatic foci (27, 28). Previously we had observed the effect of siRNA delivery by nanoparticle (25) or cobalt-poly IC nano-complexes (29) on human melanoma (A375) spheroids. Herein we tested the effect of B_4C nanoparticle on the more recognizable and morphologically distinct HeLa or B16F10 spheroids similarly. As can be seen in Figure 8, the phenotype of the 3-D tumor spheroid structures was distinct in the presence of the B_4C nanoparticles. In the case of HeLa, which were more opaque and spherical, it is easy to observe that the nanoparticle exposure causes the structures to darken from the inside out. This suggests that under these 3-D conditions simulating metastatic foci, the nanoparticles accelerate necrosis. Furthermore, conglomerates of what appears to be nanoparticle and cell-based materials are observed at the edge of the wells suggesting that nanoparticle treatment causes necrotic tissue to shed from the 3-D structure.

Discussion

Taken together the data suggest B_4C nanoparticles are able to interact with protamine:poly IC complexes. Evidence for this was shown by zeta potential and by 2-D FDS analysis. The presence of B_4C nanoparticles causes a complete lack of detecting the complexes by gel electrophoresis analysis. These data suggest that B_4C nanoparticles have a unique nanobio interface. Importantly B_4C nanoparticles inhibit the metastatic phenotype in 3-D spheroid cultures but do not effect morphology of cells grown in monolayer and show less general cytotoxicity to either NIH3T3 or A375 cells. B_4C nanoparticles had minimal effect on normal cells, shown by the hemolysis assay and by MTT assay, therefore, the anticancer effect of these particles can be attributed to the cancer phenotype. Further, the anticancer effect of B_4C nanoparticles is evident at relatively small concentrations (10-50 μg/mL) compared to the nanoparticle concentration range that is typically used in cellular studies (0-300 μg/ml) (30, 31, 32, 33, 34). These data point to the anticancer effect of B_4C nanoparticles and suggest that this may be related to their impact on protein or RNA complexes.

Acknowledgements

This work was supported by National Cancer Institute Grant 7R15CA139390-03 to RKD and LSAMP National Science Foundation Grant #1305059 to NKI. The Authors are also grateful for support from the Nanotechnology Innovation Center Kansas State (NICKS). We thank Ms. Kristin Flores and John Dean for technical assistance with the MTT assays.

References

1 Mortensen MW, Björkdahl O, Sørensen PG, Hansen T, Jensen MR, Gundersen HJG and Bjørnholm T: Functionalization and Cellular Uptake of Boron Carbide Nanoparticles. The First Step toward T Cell-Guided Boron Neutron Capture Therapy. Bioconjugate Chem *17*: 284-290, 2006.

2 Mortensen MW, Sørensen PG, Björkdahl O, Jensen MR, Gundersen HJ and Bjørnholm T: Preparation and characterization of Boron carbide nanoparticles for use as a novel agent in T cell-guided boron neutron capture therapy. Appl Radiat Isot *64*: 315-324, 2006.

3 Mortensen MW, Kahns L, Hansen T, Sorensen PG, Björkdahl O, Jensen MR, Gundersen HJ and Bjørnholm T: Next generation adoptive immunotherapy – human T cells as carriers of therapeutic nanoparticles. J Nanosci Nanotechnol *7*: 4575-4580, 2007.

4 Chattopadhyay S, Dash SK, Ghosh T, Das D, Pramanik P and Roy S: Surface modification of cobalt oxide nanoparticles using phosphonomethyl iminodiacetic acid followed by folic acid: a biocompatible vehicle for targeted anticancer drug delivery. Cancer Nanotechnol *4*: 103-116, 2013.

5 Chattopadhyay S, Dash SK, Ghosh T, Das S, Tripathy S, Mandal D, Das D, Pramanik P and Roy S: Anticancer and immunostimulatory role of encapsulated tumor antigen containing cobalt oxide nanoparticles. J Biol Inorg Chem *18*: 957-973, 2013.

6 Chung I-M, Rahuman AA, Marimuthu S, Kirthi AV, Anbarasan K and Rajakumar G: An Investigation of the Cytotoxicity and caspase-Mediated Apoptotic Effect of Green Synthesized Zinc Oxide Nanoparticles Using Eclipta prostrata on Human Liver Carcinoma Cells. Nanomater *5*: 1317-1330, 2015.

7 Priyadharshini RI, Prasannaraj G, Geetha N and Venkatachalam P: Microwave-mediated extracellular synthesis of metallic silver and zinc oxide nanoparticles using macro-algae (*Gracilaria edulis*) extracts and its anticancer activity against human PC3 cell lines. Appl Biochem Biotechnol *174*: 2777-2790, 2014.

8 Rasmussen JW, Martinez E, Louka P and Wingett DG: Zinc oxide nanoparticles for selective destruction of tumor cells and potential for drug delivery applications. Expert Opin Drug Deliv *7*: 1063-1077, 2010.

9 Liuba T, Vittoria R, Cristina R, Orazio V, Iorio MC, Vanacore R, Pietrabissa A and Cuschieri A: Zinc oxide nanoparticles as selective killers of proliferating cells. Int J Nanomedicine *6*: 1129-1140, 2011.

10 Jiang S, Eltoukhy AA, Love KT, Langer R and Anderson DG: Lipidoid-coated iron oxide nanoparticles for efficient DNA and siRNA delivery. Nano Lett *13*: 1059-1064, 2013.
11 Hernández-Gil J, Cobaleda-Siles M, Zabaleta A, Salassa L, Calvo J and Mareque-Rivas JC: An iron oxide nanocarrier loaded with a Pt(IV) prodrug and immunostimulatory dsRNA for combining complementary cancer killing effects. Adv Healthcare Mater *4*: 1034-1042, 2015.
12 Parker-Esquivel B, Flores KJ, Louiselle D, Craig M, Dong L, Garrad R, Ghosh K, Wanekaya A, Glaspell G and DeLong RK: Association of poly I:C RNA and plasmid DNA onto MnO nanorods mediated by PAMAM. Langmuir *28*: 3860-3870, 2012.
13 Gann H, Glaspell G, Garrad R, Wanekaya A, Ghosh K, Cillessen L, Scholz A, Parker B, Warner M and Delong RK: Interaction of MnO and ZnO nanomaterials with biomedically important proteins and cells. J Biomed Nanotechnol *6*: 37-42, 2010.
14 DeLong RK, Akhtar U, Sallee M, Parker B, Barber S, Zhang J, Craig M, Garrad R, Hickey AJ and Engstrom E: Characterization and performance of nucleic acid nanoparticles combined with protamine and gold. Biomaterials *30*: 6451-6459, 2009.
15 Sivamani E, DeLong RK and Qu R: Protamine-mediated DNA coating remarkably improves bombardment transformation efficiency in plant cells. Plant Cell Rep *28*: 213-221, 2009.
16 Medberry P, Dennis S, Van Hecke T and DeLong RK: pDNA bioparticles: comparative heterogeneity, surface, binding, and activity analyses. Biochem Biophys Res Commun *319*: 426-432, 2004.
17 Liu M, Feng B, Shi Y, Su C, Song H, Cheng W and Zhao L: Protamine nanoparticles for improving shRNA-mediated anti-cancer effects. Nanoscale Res Lett *10*: 134-140, 2015.
18 Yoo H and Mok H: Evaluation of multimeric siRNA conjugates for efficient protamine-based delivery into breast cancer cells. Arch Pharm Res *38*: 129-136. 2015.
19 Sköld AE, van Beek JJP, Sittig SP, Bakdash G, Tel J, Schreibelt G and de Vries IJM: Protamine- stabilized RNA as an ex vivo stimulant of primary human dendritic cell subsets. Cancer Immunol Immunother *64*: 1461-1473, 2015.
20 Cheng Y-S and Xu Feng: Anticancer function of polyinosinicpolycytidylic Acid. Cancer Biol Ther *10*: 1219-1223, 2010.
21 Zhang Y, Sun R, Liu B, Deng M, Zhang W, Li Y, Zhou G, Xie P, Li G and Hu J: TLR3 activation inhibits nasopharyngeal carcinoma metastasis *via* down-regulation of chemokine receptor CXCR4. Cancer Biol Ther *8*: 1826-1830, 2009.
22 Guillerey C, Chow MT, Miles K, Olver S, Sceneay J, Takeda K, Möller A and Smyth MJ: Toll-like receptor 3 regulates NK cell responses to cytokines and controls experimental metastasis. Oncoimmunology *4*: e1027468, 2015.
23 Forte G, Rega A, Morello S, Luciano A, Arra C, Pinto A and Sorrentino R: Polyinosinic-polycytidylic acid limits tumor outgrowth in a mouse model of metastatic lung cancer. J Immunol *188*: 5357-5364, 2012.
24 Zhou Q and Robert K: DeLong, Introductory Experiments on Biomolecules and their Interactions, 1st Edition. Academic Press c2015.
25 Delong RK, Risor A, Kanomata M, Laymon A, Jones B, Zimmerman SD, Williams J, Witkowski C, Warner M, Ruff M, Garrad R, Fallon JK, Hickey AJ and Sedaghat-Herati R: Characterization of biomolecular nanoconjugates by high-throughput delivery and spectroscopic difference. Nanomedicine (Lond) *7*: 1851-1862, 2012.
26 Reyes-Reveles J, Sedaghat-Herati R, Gilley DR, Schaeffer AM, Ghosh KC, Greene TD, Gann HE, Dowler WA, Kramer S, Dean JM and Delong RK: mPEG-PAMAM-G4 nucleic acid nanocomplexes: enhanced stability, RNase protection, and activity of splice switching oligomer and poly I:C RNA. Biomacromolecules *14*: 4108-4115, 2013.
27 Carver K, Ming X and Juliano RL: Tumor cell-targeted delivery of nanoconjugated oligonucleotides in composite spheroids. Nucleic Acid Ther *24*: 413-419, 2014.
28 Carver K, Ming X and Juliano RL: Multicellular tumor spheroids as a model for assessing delivery of oligonucleotides in three dimensions. Mol Ther Nucleic Acids *3*: e153, 2014.
29 Venuturumilli S, Dean JM, Hurst M and DeLong RK: Polyacrylic and nucleic acid cobalt hexamine nanocomplexes: characterization, RNase protection and inhibition of *in vitro* tumorigenicity in soft agar. Nanosci Nanotechnol Lett *6*: 976-981, 2014.
30 Costa C, Brandão F, Bessa MJ, Costa S, Valdiglesias V, Kiliç G, Fernández-Bertólez N, Quaresma P, Pereira E, Pásaro E, Laffon B and Teixeira JP: *In vitro* cytotoxicity of superparamagnetic iron oxide nanoparticles on neuronal and glial cells. Evaluation of nanoparticle interference with viability tests. J Appl Toxicol *36*: 361-372, 2016.
31 Orlando A, Colombo M, Prosperi D, Gregori M, Panariti A, Rivolta I, Masserini M and Cazzaniga E: Iron oxide nanoparticles surface coating and cell uptake affect biocompatibility and inflammatory responses of endothelial cells and macrophages. J Nanopart Res *17*: 351-363, 2015.
32 Gholami A, Rasoul-amini S, Ebrahiminezhad A, Seradj SH and Ghasemi Y: Lipoamino Acid Coated Superparamagnetic Iron Oxide Nanoparticles Concentration and Time Dependently Enhanced Growth of Human Hepatocarcinoma Cell Line (Hep-G2). J Nanomater *150*: 451405-451413, 2015.
33 Khan S, Ansari AA, Khan AA, Ahmad R, Al-Obaid O and Al-Kattan W: *In vitro* evaluation of anticancer and antibacterial activities of cobalt oxide nanoparticles. J Biol Inog Chem *20*: 1319-1326, 2015.
34 Chattopadhyay S, Dash SK, Ghosh T, Das S, Tripathy S, Mandal D, Das D, Pramanik P and Roy S: Anticancer and immunostimulatory role of encapsulated tumor antigen containing cobalt oxide nanoparticles. J Biol Inorg Chem *18*: 957-973, 2013.

Received March 3, 2016
Revised April 12, 2016
Accepted April 13, 2016